JOURNAL OF GUIDANCE, CONTROL, AND DYNAMICS
Vol. 17, No. 6, November–December 1994

Direct-Lift Design Strategy for Longitudinal Control of Hypersonic Aircraft

Phuong Vu* and Daniel J. Biezad†
California Polytechnic State University, San Luis Obispo, California 93407

A longitudinal control design called the G-command, alpha follow-up is described that significantly improves the lag between pitch angle and flight-path angle responses associated with hypersonic flight. The design technique relies on classical, successive loop closures to determine the control architecture and introduces a direct-lift control strategy to design dynamic compensation. This dynamic compensation constrains and "washes out" body-flap input to avoid excessive flap deflection and associated heating while providing angle-of-attack control at the engine inlet. The final design was implemented on a generic hypersonic aircraft simulation at NASA Dryden and evaluated by a NASA test pilot familiar with the SR-71. The pilot flew turning and altitude change maneuvers using the implemented control law and verified the ability to track flight path with ease and precision. Finally, evidence is presented that supports a flying qualities metric for longitudinal, hypersonic flight based on the bandwidth of the flight-path-angle-to-stick-frequency response.

Introduction

LONGITUDINAL control of a hypersonic vehicle (HSV) flight path, even in "equilibrium" flight, presents a nonlinear, time-varying problem of enormous complexity. Equilibrium itself is difficult to define for hypersonic flight, powered or unpowered, and for modeling purposes "equilibrium" is typically replaced by a "nominal" ascent or descent trajectory where forward acceleration or deceleration is held constant and where nonrotating, flat-Earth assumptions used to derive subsonic aircraft equations of motion no longer apply.[1]

These trajectories for ascent or descent of a hypersonic vehicle are vitally important, and a major concern is often the precise control of flight path. Attaining this precision is inhibited by the long time lag ($T_{\theta 2}$) between the pitch attitude and flight-path responses, which also adversely affects handling qualities. Control of the flight path using pitch attitude is adequate when the flight-path-to-pitch-attitude time lag $T_{\theta 2}$ is less than 5 s, but in the hypersonic aircraft it can exceed 60 s. Variants of pitch rate designs for hypersonic vehicles have used prefilters to overdrive the pitch rate in order to improve the path response bandwidth.[2]

Control is further complicated by the large, lifting bow wave under the vehicle, by the airframe-to-engine coupling inherent in HSV design, and by the amplified effects of static margin changes with Mach number.[3] These effects require, in addition to precise flight-path control, that other key control issues be addressed early in the design process. These issues include high temperatures, which place strict limits on control surface activity, and thrust-to-airframe coupling, which demands that the control system constrain large transient fluctuations of the angle of attack at the engine inlet. Conventional subsonic designs that feed back normal acceleration to the elevons (usually with inner pitch rate loops) may cause excessive variations in angle of attack at the engine inlet. A control system that does not actively control the engine inlet conditions can allow the engines to flame out even during simple and basic maneuvers, such as level off from a climb.

Proper selection of control architecture, therefore, is most important. Many control strategies are possible, but the architecture chosen here focuses on the key hypersonic issues discussed above and is justified in a step-by-step manner for practical implementation. Given the architecture, the compensation is obtained by classical means. The resulting design reduces $T_{\theta 2}$ without prolonging body-flap deflection δ_{BF} and exhibits good handling qualities, as will be explained in the pilot evaluation section.

This study focuses only on longitudinal control. The generic hypersonic model used by NASA is first presented, followed by a discussion of the control strategy required to precisely control both flight-path and engine inlet conditions while constraining control deflections. The G-command, alpha follow-up (GAF) design procedure is then briefly reviewed, with emphasis on the direct-lift implementation and the dynamic compensation between the flaps and elevons. The resulting system may be considered a minimal stability and control augmentation system (SCAS) as presented to the pilot.[4] In the final sections the results of a piloted flight evaluation are presented and evidence is given for a hypersonic flying qualities metric based on flight-path-to-stick bandwidth. Phugoid and density modes are not considered in the flying qualities analysis because it is presumed that the pilot will be actively in the control loop.

Hypersonic Vehicle and Control Strategy

NASA Generic Hypersonic Aerodynamic Model Example

The Generic Hypersonic Aerodynamic Model Example (GHAME) is a model developed by NASA[5] intended to provide universities and government agencies with a realistic and unclassified model of a single-stage-to-orbit (SSTO) vehicle. A side view of the model is shown in Fig. 1. It has a gross take-off weight of 300,000 lb and a dry weight of 120,000 lb. It is a 70-deg delta-wing configuration with a single vertical tail and mixed ailerons and elevators. The vehicle is 243 ft long with a span of 80 ft and area of 6000 ft^2. The fuselage from front to back consists of a 10-deg half-angle cone ending in a 20-ft-diam cylinder ending in an integrated boat-tail/nozzle.

To implement the direct-lift control scheme, body flaps similar to those on the Space Shuttle were added to the GHAME. The flaps were sized to produce a 1-g response for full deflection at Mach 3 and dynamic pressure (Q-bar) of 954 psf. The control limits are

$$-22 \text{ deg} < \delta_e < 22 \text{ deg} \qquad 0\% < \delta_T < 100\%$$

$$-12 \text{ deg} < \delta_{BF} < 22 \text{ deg}$$

The location of the body flaps was largely determined by the available math model. When feasible, actual direct-lift controls would be placed near the center of gravity. The body-flap location in the case presented here is thus not optimal for control design. It is also

Presented as Paper 93-3814 at the AIAA Guidance, Navigation, and Control Conference, Monterey, CA, Aug. 9–11, 1993; received June 16, 1993; revision received Jan. 27, 1994; accepted for publication May 7, 1994.

*Graduate Research Assistant, Aeronautical Engineering Department. Student Member AIAA.

†Professor, Aeronautical Engineering Department. Associate Fellow AIAA.

Table 1 Design conditions and dynamics

Q-bar	Mach 3	Mach 6	Mach 10
Low	Q-bar = 502 psf $M_\alpha = -0.459$ $T_{\theta 2} = 11.3$ s	Q-bar = 502 psf $M_\alpha = -0.357$ $T_{\theta 2} = 50$ s	Q-bar = 501 psf $M_\alpha = -0.448$ $T_{\theta 2} = 91$ s
Medium	Q-bar = 954 psf $M_\alpha = -0.974$ $T_{\theta 2} = 3$ s	Q-bar = 1004 psf $M_\alpha = -0.731$ $T_{\theta 2} = 7$ s	Q-bar = 1042 psf $M_\alpha = -0.993$ $T_{\theta 2} = 66$ s
High	Q-bar = 1503 psf $M_\alpha = -1.689$ $T_{\theta 2} = 2$ s	Q-bar = 1499 psf $M_\alpha = -1.495$ $T_{\theta 2} = 8$ s	Q-bar = 1523 psf $M_\alpha = -1.501$ $T_{\theta 2} = 13$ s

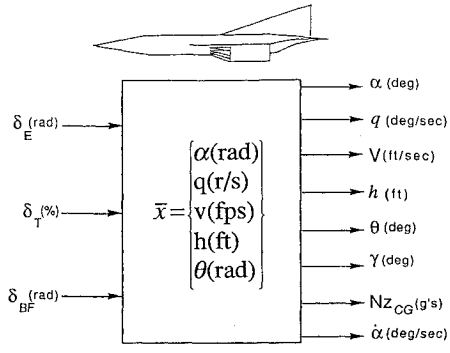

Fig. 1 GHAME modified with body flaps.

important to note that the important considerations of rate limits and hinge moment limits of a body-flap actuator are not analyzed.

Hypersonic Model Response

The longitudinal flight dynamics of the GHAME are shown in Fig. 1. Nine representative powered-flight points in the flight envelope were obtained as summarized in Table 1, and linearizations using state-space quadruples were entered into a controls analysis program.[6] The state-space representation used to illustrate the control system design that follows is shown in the Appendix for the Mach 3, dynamic pressure, 954-psf (Q-bar) powered configuration at 60,000 ft pressure altitude. Note from the Appendix that feedforward exists for N_{zcg} and that the units for some states change from radians to degrees at the output. The complete set of representations may be found in Ref. 7.

A system survey as described in Ref. 8 (p. 189) was accomplished for all of the linearized models. Sets of 10-s time responses from the state-space quadruple representing the Mach 3, Q-bar 954-psf configuration are shown in Fig. 2 (long-period mode effects would require much longer time scales to be observed). The elevons rotate the vehicle to about 14 deg pitch attitude and 8 deg alpha within 4 s. The flight path trails the pitch attitude and reaches 14 deg in 10 s. This indicates a flight-path-to-attitude lag of 6 s, exhibiting the low $C_{L\alpha}$ characteristic of the GHAME. The elevons' obvious importance is in controlling pitch and angle of attack, but the g response is slow.

The vehicle response to a 10-deg step input of body flaps produces negative moments and an adverse negative angle of attack. However, note the resulting normal acceleration, N_{zcg}, which has a much faster rise time than the g due to an elevon step. This rapid initial response, due to the feedforward link between body flaps and N_{zcg} (see Appendix), is exploited in the direct-lift strategy that follows to reduce the large flight-path-to-attitude lag. Note also that the bare airframe response does not include actuators for the body flaps.

The vehicle response to a step throttle input ($\delta_t = 10\%$) shows that the vehicle pitches down (negative Cm_u) with negative angles of attack even though the flight-path angle increases. Feedback to the throttles to alleviate the pitch down is discussed in Ref. 7 but was not considered in the GAF design.

GAF Control Strategy

The GAF system design is an attempt to address three key requirements of hypersonic flight: precise flight-path control (to eliminate the long lag, $T_{\theta 2}$, between the pitch attitude and flight-path responses); precise angle-of-attack control at the engine inlet (to reduce the adverse effects of engine/airframe coupling); and the limiting and "washing out" of body-flap deflection (to alleviate the heat loading).

By feeding back the normal acceleration (N_{zcg}) to the body flaps, the pilot in effect commands normal g values in a way that exploits the rapid response to body-flap control. With the body flaps deflected there is an increase in lift, but also a pitch-down moment due to the rearward shift in the center of pressure. To avoid the resulting pitch down, an interconnect is made from the body flaps to the elevons. Its purpose is to counteract the moment generated by the body flaps with that of the elevons in a "follow-up" strategy. Maneuvers that require holding constant g values for an extended period of time, such as steady level turns and long climbs, would place severe heating stresses on the deflected flaps.[9] The aim is therefore to "wash out" the body flaps and at the same time retain the commanded g values by increasing lift using the elevons to control the angle of attack.

Direct-Lift Control Design

GAF Design

The GAF design was implemented for nine different flight conditions, as summarized in Table 1 and as documented in Refs. 7 and 10. The choice of Mach 10 as the upper bound was justified by the Mach number independence principle for aerodynamic coefficients.[11] During the design of the GAF scheme the long-period modes (density and phugoid) are neglected and it is assumed that the control law parameters vary slowly between the linear design points so that gain scheduling can be used.[12,13] In effect the compensators are designed based on the short-period model.

Design Steps

There are five steps in the pseudoloop GAF design. The steps are presented below using the powered configuration described in the Appendix.

Step 1. Based on the system survey, select a primary controller based on the primary task for the pilot, which in this case is g control (or altitude rate) using body-flap deflection. As previously discussed, selection of the elevon as primary controller would cause large pitch and angle-of-attack rates in order to attain adequate $T_{\theta 2}$.

Models for the actuators and the zero-order hold (ZOH) are appended in front of the body flaps and elevons, including a conversion factor from degrees to radians. The ZOH model is added to represent the lag introduced by the computer simulation 50-H cycle time. The conversion factor, actuator, and ZOH are lumped into a transfer function named GX (see the lower left panel of Fig. 3). As a practical note, the fast body-flap actuator may be prohibitively expensive, and there are important concerns regarding rate and hinge moment limits for this type of actuator that are not addressed here.

Step 2. A crossfeed gain (K95 = 0.43 in Fig. 3) is made from the body flaps to the elevons to negate the moments from the body flaps and is close to $C_{M\delta_{BF}}/C_{M\delta_E}$. Given more design freedom the body flaps would be located closer to the vehicle center of gravity and reduce the need for this crossfeed.

Step 3. The next task is to design the α-stabilizing loop so that it is effective in the low- to midfrequency ranges. This is done by feeding back $\dot{\alpha}$ to the elevons command, δ_{ec}. The open-loop Bode diagram (not shown) for the $\dot{\alpha}/\delta_{ec}$ transfer function indicates the loop will be inactive below 1 rad/s and thus be sensitive at low frequencies to parameter variations. Increasing the system "type" with a proportional-and-integral (PI) compensator improves the loop shape below and near crossover and increases the effectiveness of this feedback loop.[8] The PI compensator, PI85 $= 2(s+1)/s$, yields dominant roots with short-period damping of 0.7 (note that sensor feedback of $\dot{\alpha}$ is currently impractical, in some cases estimated or reconstructed from other states in selected frequency ranges).

Step 4. The next step in controlling the angle-of-attack response is to feed back α itself. The frequency response prior to closing the α loop for $\alpha/\dot{\alpha}_c$ is shown in the top left panel of Fig. 3. Stability margins (PM = 87 deg and GM = 23 dB) are adequate with type 1 system behavior at the lower frequencies. The gain K16 is set at 0.7 (top right panel of Fig. 3) to provide a fast, nonoscillatory response

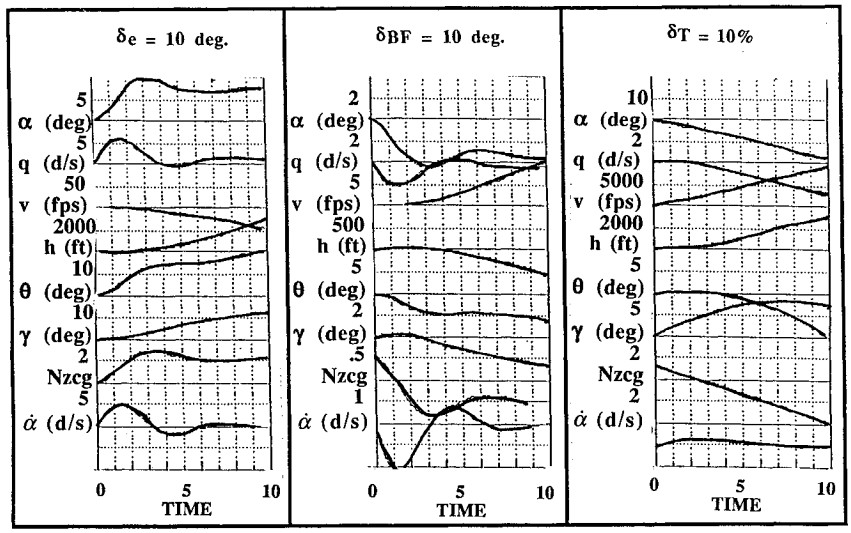

Fig. 2 Bare airframe time responses.

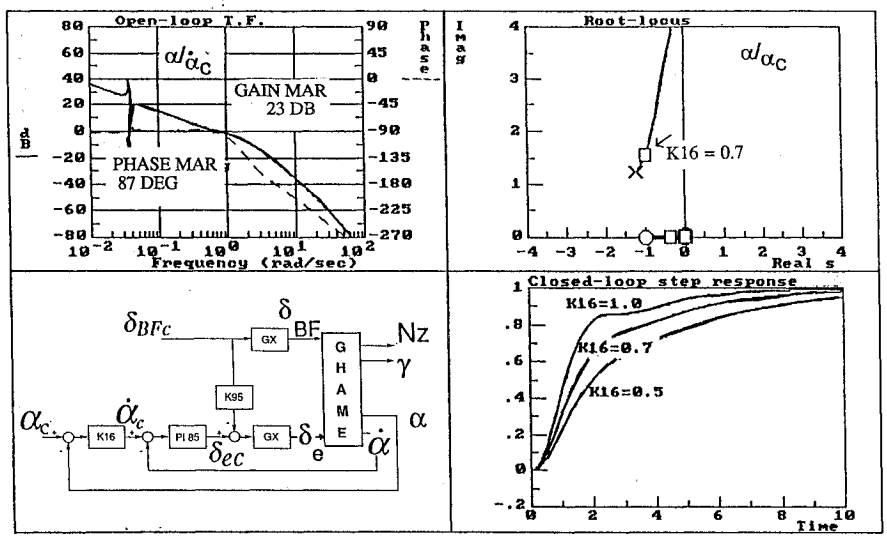

Fig. 3 System survey for $\alpha/\dot{\alpha}_c$.

yet allow for gain scheduling variation. This extremely important loop is the essence of the "alpha follow-up" scheme. It ensures the proper inlet conditions for the engines, constrains large transient changes in α, and will wash out the body flaps (with an interconnect explained in the next step).

Step 5. The primary control loop in the GAF scheme feeds back normal acceleration (N_{zcg}) through a PI compensator [PI74 = $15(s+10)/s$] as shown in Fig. 4. This compensator shapes the N_z/δ_{BFc} frequency response (not shown) by boosting the gain and removing a "shelf" for $\omega = 0.1, \ldots, 10$ rad/s. The gain of 15 was set to provide a crossover frequency of 10 rad/s. The stick signal is reduced through the gain (K79 = 0.18) to provide 1 g in the steady state for a stick deflection of 5.5 in. Figure 5 shows the vehicle time response to a step stick input of $\delta_S = 5.5$ in. Notice that, following the initial peak of 22 deg or 0.38 rad for the body flaps, the flap deflection has the undesirable property of slowly increasing with time.

As discussed above, maneuvers requiring sustained 'g' values (such as steady turns) are prone to actuator saturation and heat loading on the body flaps. Alpha follow-up is now added, as shown in Fig. 4, by connecting δ_{BFc} and α_C through compensator PI137. This is done to wash out the body flaps and to prevent saturation and excessive heating. An approximate wash-out time constant of 20 s for the body flaps is obtained by implementing

$$\text{PI137} = -0.02(s + 1.0)/s$$

The details are explained in Ref. 14.

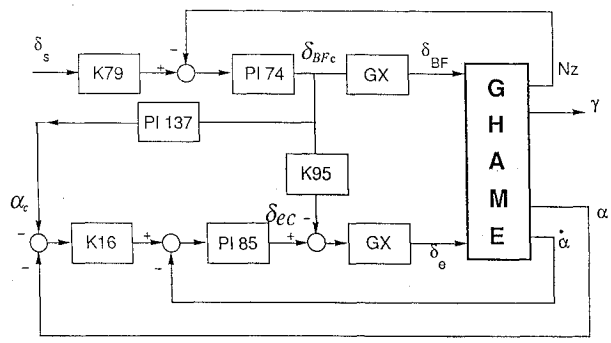

Fig. 4 Final architecture selection with stick-limiting gain.

The vehicle response for the final design to a maximum stick deflection is shown in Fig. 6 (commanded $N_{zcg} = 1.0$). This response is initiated by the flaps whose effects are subsequently replaced by the slowly increasing angle of attack through the alpha follow-up, hence the term g command, alpha follow-up. The resulting system constrains angle of attack and controls altitude rate (g command), permanently altering airframe dynamics as presented to the pilot to improve response time and handling qualities.

Parameter Scheduling

The above steps were repeated for eight other flight conditions, and a matrix of the controller variables relating Mach number and

Table 2 Design conditions and compensation

Q-bar	Mach 3	Mach 6	Mach 10
Low	Q-bar = 502 psf	PQ-bar = 502 psf	Q-bar = 501 psf
	$K[95] = 0.37$ (0.4)	$K[95] = 0.26$ (0.25)	$K[95] = 0.19$ (0.17)
	$K[85] = -2.6$ (−2.6)	$K[85] = -2.0$ (−2.6)	$K[85] = -2.6$ (−2.6)
	$\omega[85] = 0.7$ (0.7)	$\omega[85] = 0.6$ (0.7)	$\omega[85] = 0.7$ (0.7)
	$K[16] = 0.6$ (0.5)	$K[16] = 0.5$ (0.5)	$K[16] = 0.5$ (0.5)
	$K[74] = 22$ (25.5)	$K[74] = 50$ (46.4)	$K[74] = 70$ (74.3)
	$K[79] = 0.1$ (0.1)	$K[79] = 0.05$ (0.049)	$K[79] = 0.031$ (.031)
	$\omega[137] = 1.0$ (0.99)	$\omega[137] = 0.7$ (0.83)	$\omega[137] = 0.5$ (0.62)
Medium	Q-bar = 954 psf	Q-bar = 1004 psf	Q-bar = 1042 psf
	$K[95] = 0.43$ (0.4)	$K[95] = 0.24$ (0.25)	$K[95] = 0.17$ (0.17)
	$K[85] = -2.0$ (−2.02)	$K[85] = -1.2$ (−1.96)	$K[85] = -1.6$ (−1.91)
	$\omega[85] = 1.0$ (0.92)	$\omega[85] = 0.8$ (0.95)	$\omega[85] = 1.0$ (0.96)
	$K[16] = 0.7$ (0.6)	$K[16] = 0.6$ (0.6)	$K[16] = 0.7$ (0.61)
	$K[74] = 15$ (15.8)	$K[74] = 25$ (26.1)	$K[74] = 40$ (39.1)
	$K[79] = 0.18$ (0.18)	$K[79] = 0.1$ (0.11)	$K[79] = .064$ (.062)
	$\omega[137] = 1.0$ (0.99)	$\omega[137] = 0.8$ (0.83)	$\omega[137] = 0.7$ (0.62)
High	Q-bar = 1503 psf	Q-bar = 1499 psf	Q-bar = 1523 psf
	$K[95] = 0.4$ (0.4)	$K[95] = 0.23$ (0.25)	$K[95] = 0.16$ (0.17)
	$K[85] = -1.4$ (−1.33)	$K[85] = -1.2$ (−1.33)	$K[85] = -1.3$ (−1.3)
	$\omega[85] = 1.4$ (1.19)	$\omega[85] = 1.3$ (1.19)	$\omega[85] = 1.2$ (1.2)
	$K[16] = 0.8$ (0.7)	$K[16] = 0.8$ (0.7)	$K[16] = 0.7$ (0.7)
	$K[74] = 10$ (11.8)	$K[74] = 20$ (19.1)	$K[74] = 25$ (28.4)
	$K[79] = 0.18$ (0.18)	$K[79] = 0.16$ (0.163)	$K[79] = 0.091$ (.093)
	$\omega[137] = 1.0$ (0.99)	$\omega[137] = 1.0$ (0.83)	$\omega[137] = 0.7$ (0.62)

Note: Numbers in parentheses are scheduled gains. Compensator form from Fig. 7: PI[#] = K[#] $(s + \omega[\#])/s$.

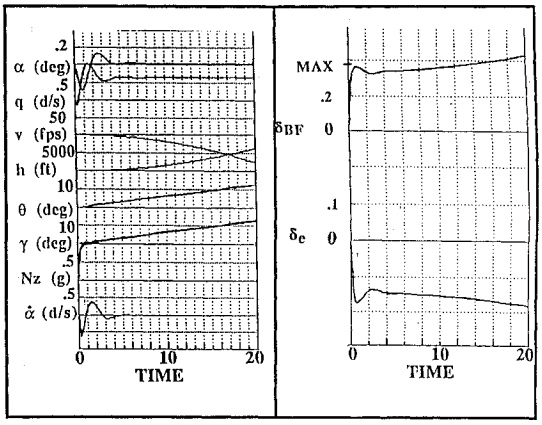

Fig. 5 Time responses without alpha follow-up.

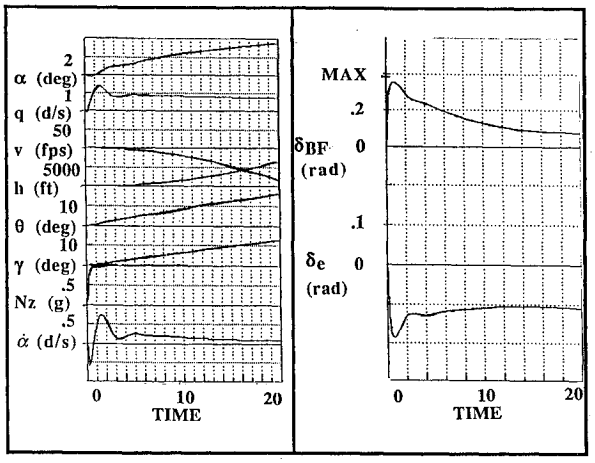

Fig. 6 Time responses of final design.

dynamic pressure (Q-bar) is summarized in Table 2. A schedule was determined for each parameter from the linear designs using simple analytic functions of Mach and dynamic pressure. The controllers were digitized with the Tustin transformation and implemented in a simulation, the details of which are described in Ref. 7 and 10. Batch results of the nonlinear simulation at NASA were verified at the nine design points for small control inputs before the piloted simulation described next.

Pilot Evaluation

The GAF scheme was implemented on the nonlinear GHAME simulation at NASA Dryden and evaluated by a NASA test pilot familiar with the SR-71. He was asked to perform steady, level turns and vertical plane altitude change maneuvers without being briefed on the flight control implementation. The pilot was presented with a standard heads-up display without pitch steering command bars. Vertical bars indicating altitude, vertical speed, and normal acceleration were on the instrument panel.

In general, up-and-away flying required little effort, and the pilot workload was minimal. The capability to track flight-path angle precisely was verified by pilot comments. Although numerical Cooper-Harper ratings were not assigned by the pilot, pilot comments and performance relative to SR-71 specifications indicated that the GAF scheme results in a level 1 flight vehicle.

Turning Maneuvers

The pilot was asked to perform level turns at 30 deg of bank for trimmed flight conditions and performance specifications (taken from SR-71 requirements), as depicted in Table 3. The turns were accomplished with little difficulty. The pilot commented that, once inside the turn, holding a constant altitude was a simple matter of driving the vertical velocity to zero. Since the GAF scheme has an alpha-stabilizing loop, the vehicle tends to roll about its velocity vector. This caused the pilot to comment that the vehicle consistently undershot the target heading by 3 or 4 deg.

Vertical Plane Altitude Change

The pilot was asked to perform aggressive altitude changes from trimmed flight conditions as depicted in Table 4. The pilot was briefed to accomplish the altitude change maneuvers at 5000 fpm for the Mach 3 condition and 10,000 fpm at the higher Mach numbers.

The qualitative results of the piloted evaluations for the aggressive altitude changes are summarized in Table 4. There was concern about leveling off at the Mach 10 condition where full-forward stick was reached, but no adverse comments were made about the control of attitude. The body flaps could not produce enough force to overcome the high rate of climb and the centripetal force (which is

Table 3 Performance specifications (SR-71)

Flight condition	Controlled parameter	Adequate performance	Desired performance
Mach 3, altitude 60,000 ft	Target heading (8 deg)	±2 deg	±1 deg
	Target altitude	±20 knots	±10 knots
Mach 6, altitude 90,000 ft	Target heading (4 deg)	±1 deg	±0.5 deg
	Target altitude	±600 ft	±200 ft
	Trim KEAS	±20 knots	±10 knots
Mach 10, altitude 110,000 ft	Target heading (2 deg)	±1 deg	±0.5 deg
	Target altitude	±1000 ft	±300 ft
	Trim KEAS	±20 knots	±10 knots

Abbreviation: KEAS, knots equivalent air speed.

Table 4 Pilot comment summary

Mach number	Altitude, ft	Altitude change, ft	Vertical speed, fpm	Comments
3	60,000	5,000	5,000	Can get within 400 ft of target altitude. Sluggish initial response, but representative. Response is predictable. An aggressive maneuver for the SR-71. H-dot (flight path) is easy to maintain.
6	90,000	−10,000	−10,000	Can get within 1000 ft of target altitude. A very, very aggressive maneuver. Response is realistic.
6	90,000	10,000	10,000	Overshot target altitude by 400 ft. 80 fps (5000 fpm) is more representative of the desired rate of climb. Response is similar to the SR-71.
10	110,000	20,000	10,000	Run out of forward stick in climb when trying to come out/level off, while climbing at 80 fps. Push-over is "OK" at 32 fps (2000 fpm). H-dot (flight path) is very easy to get.

significant at the higher Mach numbers). Adequate control power for leveling off from an aggressive climb is a legitimate concern. The allowable rates of climb at different flight conditions should be an essential specification in determining the hypersonic flight envelope.

The pilot recommended that the vertical speed bars on the instrument panel be relocated to the heads-up display. He suggested the need for command pitch steering to help control altitude (the closed-loop control of altitude is K/s^2 for a g command system) but did not experience any pilot-induced oscillations. He also noted that the GAF control system was a vast improvement over the existing pitch rate command system.

Hypersonic Flying Qualities Metrics

The GAF-controlled GHAME is a direct-lift control vehicle, frequently referred to as control-configured vehicles (CCVs). The unconventional responses of such aircraft exceed the scope of flying qualities specifications[15] and the existing data base for evaluating such aircraft is sparse. It has been proposed that the criteria for such aircraft include the bandwidth of the open-loop transfer function between the output the pilot is controlling and the stick.[16]

Since the GAF control system is a minimal SCAS, open loop implies that the stability and control augmentation is operating when the bandwidth is measured. This bandwidth is defined as the lowest frequency for which the open-loop phase margin is at least 45 deg and the gain margin is at least 6 dB (see Ref. 15). Since flight-path tracking dominates the category B flight phase of the GHAME vehicle, it can be hypothesized that the bandwidth based on the γ/δ_S transfer function is a more appropriate evaluation tool than is the θ/δ_S attitude bandwidth in current handling qualities specifications.

To test this hypothesis, pitch rate command systems were developed for the nine configurations of Table 1. No attempt was made, however, to optimize the flight-path designs relative to $T_{\theta 2}$. A bandwidth comparison between the GAF and pitch rate designs (QCOM) for this configuration is shown in Fig. 7. The top panels of Fig. 7 show

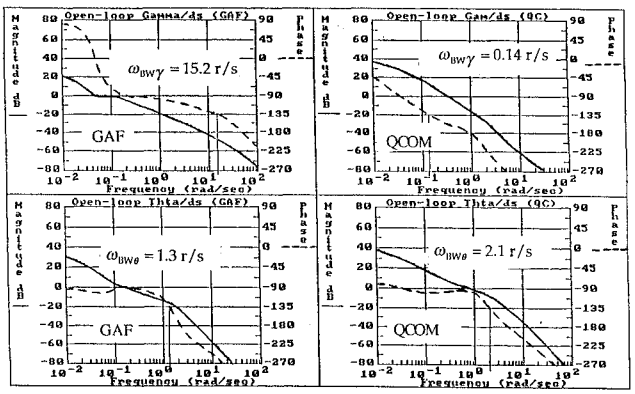

Fig. 7 GAF and QCOM bandwidths for Mach 3, Q-bar 954 psf, altitude 60,000 ft.

that the bandwidth based on flight-path angle, $\omega_{BW\gamma}$, for the GAF design (left side, $\omega_{BW\gamma} = 15.2$ rad/s) is two orders of magnitude larger than that for the QCOM design (right side, $\omega_{BW\gamma} = 0.14$ rad/s). Conversely, the bottom panels of Fig. 7 show that the bandwidth based on attitude, $\omega_{BW\theta}$, is larger for the QCOM design ($\omega_{BW\theta} = 2.1$ rad/s) than for the GAF design ($\omega_{BW\theta} = 1.3$ rad/s).

Based on the piloted evaluation of the GAF-controlled GHAME and the same pilot's unfavorable experience with the GHAME's original pitch rate system, there is evidence that a handling qualities metric based on $\omega_{BW\gamma}$ may be more appropriate for hypersonic flight than one based on $\omega_{BW\theta}$. This is further substantiated by the data in Fig. 8. Here the $\omega_{BW\gamma}$ for each of nine QCOM designs, shown by the plus signs, can be seen to be much smaller than the $\omega_{BW\gamma}$ from the GAF designs for the other eight configurations of Table 1, shown by circles. None of these configurations received pilot ratings, and so the "levels," superimposed from Ref. 15, are shown for illustrative purposes only.

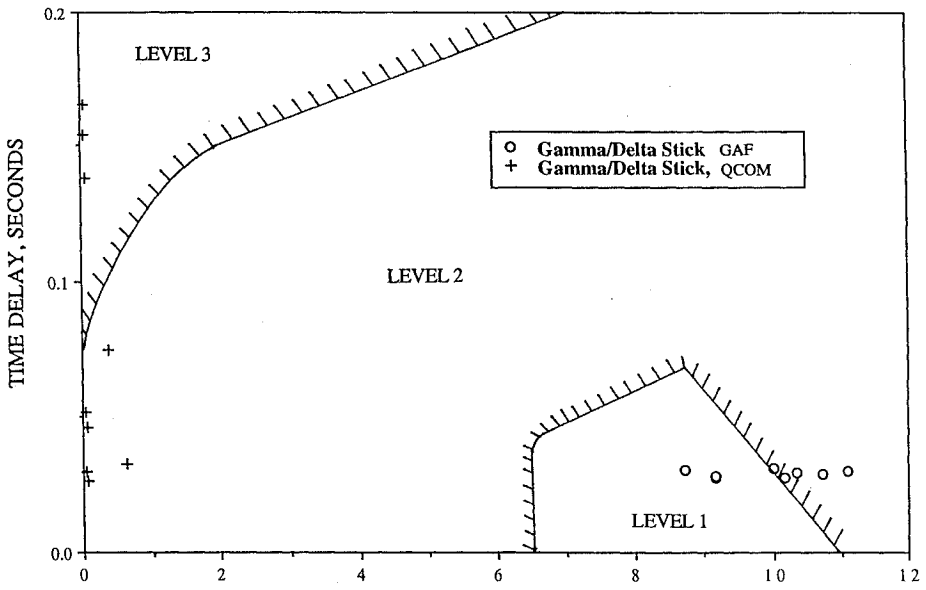

Fig. 8 Handling qualities $\omega_{BW\gamma}$ bandwidth comparisons of GAF and QCOM designs.

Conclusions

The GAF control strategy significantly reduces the path-to-attitude time lag by employing both body flaps and elevons for path control. A stick step input initiates the g response using body-flap deflections, which are then washed out by the elevons while commanded g is held constant and angle of attack at the engine inlet is constrained to change slowly.

A procedure for the direct-lift, alpha follow-up design was presented. Architecture selection was based on successive loop closures and relied on intuition resulting from experience with classical design involving multiple inputs and outputs. A theoretical investigation of the stability resulting from this design technique would be useful along with its relationship to modern robust control design techniques and is recommended for future work.

A NASA test pilot flew turn and altitude change maneuvers in the simulation facility using the control design presented here on a full, nonlinear simulation to Mach numbers and dynamic pressures in excess of 20 and 2000 psf, respectively. He had no trouble controlling the pitch axis and commented that it flew similar to the SR-71. His prior experience with the unaugmented vehicle showed significant improvement in flight-path tracking. Learning was required to anticipate lead for level off and pitch steering bars were suggested to improve the accuracy. It was concluded that the direct-lift, alpha follow-up scheme was practical and robust.

A handling qualities analysis of nine flight conditions provided solid evidence on the importance of the flight-path bandwidth for hypersonic flight. An adequate database of pilot ratings for hypersonic vehicles is needed. Also, the practicality of implementing direct-lift control for hypersonic vehicles remains to be addressed. The need for a high-bandwidth direct-lift surface should be evaluated against the associated cost and presumes a requirement that the pilot will remain active in the control loop.

Although caution must be taken in generalizing the results presented here to other types of hypersonic vehicles, some aspects of the hypersonic model are generic. These characteristics include the low $C_{L\alpha}$ (translating into large $T_{\theta 2}$), the airframe-to-engine coupling, and the high temperatures of the deflected control surfaces.

Appendix: State-Space Quadruple Representation for Mach 3, Q-bar 954-psf, 60,000-ft MSL

$$\dot{x} = Ax + Bu$$

$$y = Cx + Du$$

$$x = \begin{bmatrix} \alpha(\text{rad}) \\ q(\text{rer/s}) \\ v(\text{fps}) \\ h(\text{ft}) \\ \theta(\text{rad}) \end{bmatrix} \quad u = \begin{bmatrix} \delta_e(\text{rad}) \\ \delta_T(\%) \\ \delta_{BF}(\text{rad}) \end{bmatrix} \quad y = \begin{bmatrix} \alpha(\text{deg}) \\ q(\text{deg/s}) \\ v(\text{fps}) \\ h(\text{ft}) \\ \theta(\text{rad}) \\ \gamma(\text{deg}) \\ N_{zcg}(g) \\ \dot{\alpha}(\text{deg/s}) \end{bmatrix}$$

$$\left[\begin{array}{c|c} A & B \\ \hline C & D \end{array}\right] =$$

$$\left[\begin{array}{ccccc|ccc}
-0.196 & 1.0 & -0.875 \times 10^{-6} & 0.505 \times 10^{-6} & -0.191 \times 10^{-4} & -0.256 \times 10^{-2} & -0.386 \times 10^{-2} & -0.343 \times 10^{-1} \\
-0.974 & -0.489 & -0.364 \times 10^{-4} & -0.694 \times 10^{-8} & 0.0 & -0.815 & 0.0 & -0.338 \\
23.41 & -0.674 \times 10^{-4} & -0.14 \times 10^{-1} & -0.549 \times 10^{-5} & -31.41 & 0.0 & 84.14 & -0.278 \times 10^{-4} \\
-2904 & 0.437 \times 10^{-3} & 0.173 \times 10^{-1} & -0.858 \times 10^{-7} & 2904 & 0.0 & 0.0 & 0.0 \\
0.0 & 1.0 & -0.477 \times 10^{-7} & -0.669 \times 10^{-11} & -0.417 \times 10^{-9} & 0.0 & 0.0 & 0.0 \\
\hline
57.3 & -0.137 \times 10^{-4} & -0.238 \times 10^{-7} & -0.238 \times 10^{-8} & 0 & 0 & 0 & 0 \\
0 & 57.3 & 0 & 0 & 0 & 0 & 0 & 0 \\
0.699 \times 10^{-2} & 0 & 1.0 & 0 & 0 & 0 & 0 & 0 \\
0 & 0 & 0 & 1.0 & 0 & 0 & 0 & 0 \\
0 & 0 & 0 & 0 & 57.3 & 0 & 0 & 0 \\
-57.3 & 0.122 \times 10^{-4} & 0.213 \times 10^{-7} & -0.213 \times 10^{-8} & 57.30 & 0 & 0 & 0 \\
17.55 & -0.342 \times 10^{-5} & 0.405 \times 10^{-4} & 0.455 \times 10^{-4} & 0 & 0.23 & 0.127 & 3.086 \\
-11.21 & 57.3 & -0.502 \times 10^{-4} & 0.289 \times 10^{-4} & -0.11 \times 10^{-2} & -0.146 & -0.221 & -1.966
\end{array}\right]$$

Acknowledgments

The authors are grateful to Bruce Powers and Tim Cox at NASA Dryden for their guidance and support. This work could not have been accomplished without their active participation.

References

[1]Etkin, B., "Longitudinal Dynamics of a Lifting Vehicle in a Circular Orbit," Rept. 65, Air Force Office of Scientific Research, TN 60-191, Feb. 1960.

[2]McRuer, D. T., and Myers, T. T., "Considerations for the Development of NASP Flying Qualities Specifications," Weight Aeronautics Laboratories, WL-TR-92-3042, June 1992.

[3]Myers, T. T., and Klyde, D. H., "Hypersonic Open-Loop Vehicle Analysis," Systems Technology Inc., WP 1277-9, June 1991.

[4]McRuer, D. T., Johnston, D. E., and Myers, T. T., "A Perspective on Superaugmented Flight Control: Advantages and Problems," *Journal of Guidance, Control, and Dynamics*, Vol. 9, No. 5, 1986, pp. 530–540.

[5]Bowers, A. H., Noffz, G. K., Gonda, M., and Iliff, K. W., "A Generic Hypersonic Aerodynamic Model Example (GHAME)," NASA Internal Memo, TM, Aug. 1989.

[6]Thompson, P. M., *Program CC Version 4 Tutorial and User's Guide*, Systems Technology Inc., Hawthorne, CA, Nov. 1988.

[7]Vu, P. T., "Design of a Flight Path Controller for a Hypersonic Aircraft," M.S. Thesis, Aeronautical Engineering Department, California Polytechnic State Univ., April 1993.

[8]McRuer, D., Ashkenas, I., and Graham, D., *Aircraft Dynamics and Automatic Control*, Princeton Univ. Press, Princeton, NJ, 1973.

[9]Neumann, R. D., "Defining the Aerothermodynamic Methodology," in *Hypersonics, Vol. I: Defining the Hypersonic Environment*, edited by J. J. Bertin, R. Glowinski, and J. Periaux, Birkhäuser, Boston, 1989.

[10]Vu, P. T., and Biezad, D. J., "Longitudinal Control of Hypersonic Aircraft: An Alpha Follow-Up Scheme," *Proceedings of the First IEEE Regional Conference on Aerospace Control Systems* (Westlake Village, CA), Inst. of Electrical and Electronics Engineers, Piscataway, NJ, May 1993, pp. 440–444.

[11]Bertin, J. J., "General Characterization of Hypersonic Flows," in *Hypersonics, Vol. I: Defining the Hypersonic Environment*, edited by J. J. Bertin, R. Glowinski, and J. Periaux, Birkhäuser, Boston, 1989.

[12]Astrom, K. J., and Wittenmark, B., *Adaptive Control*, Addison-Wesley, Reading, MA, 1989.

[13]Shamma, J. S., and Athans, M., "Gain Scheduling: Potential Hazards and Possible Remedies," *IEEE Control Systems Magazine*, Vol. 12, No. 3, June 1992, pp. 101–107.

[14]Vu, P. T., and Biezad, D. J., "A Pseudo-Loop Design Strategy for the Longitudinal Control of Hypersonic Aircraft," *Proceedings of the AIAA Guidance, Navigation, and Control Conference* (Monterey, CA), AIAA, Washington, DC, 1993, pp. 1021–1028.

[15]"Flying Qualities of Piloted Vehicles," MIL-STD-1797A(ASG), ASD/ENES, Wright-Patterson AFB, OH, Jan. 1990.

[16]Hoh, R. H., Myers, T. T., Ashkenas, I. L., Ringland, R. F., and Craig, S. J., "Development of Handling Qualities Criteria for Aircraft with Independent Control of Six Degrees of Freedom," TR-81-3027, AFWAL, Wright-Patterson AFB, OH, April 1981.